

NASA Technical Memorandum 84469

FOR REFERENCE

NASA-TM-84469 19830004086

NOT TO BE TAKEN FROM THIS ROOM

**INTEGRATED FINITE ELEMENT THERMAL-STRUCTURAL
ANALYSIS WITH RADIATION HEAT TRANSFER**

**EARL A. THORNTON, PRAMOTE DECHAUMPHAI AND
ALLAN R. WIETING**

SEPTEMBER 1982

LIBRARY COPY

SEP 29 1982

**LANGLEY RESEARCH CENTER
LIBRARY, NASA
HAMPTON, VIRGINIA**



**National Aeronautics and
Space Administration**

**Langley Research Center
Hampton, Virginia 23665**

INTEGRATED FINITE ELEMENT THERMAL-STRUCTURAL ANALYSIS WITH RADIATION HEAT TRANSFER

Earl A. Thornton and Pramote Dechaumphai
Old Dominion University
Norfolk, Virginia

and

Allan R. Wieting
NASA Langley Research Center
Hampton, Virginia

Abstract

An integrated approach for efficiently coupling thermal and stress analyses of structures with radiation heat transfer is presented. A new integrated one dimensional element based on a nodeless variable formulation is introduced. Lumped and consistent formulations of the nonlinear radiation heat transfer matrix are presented. The accuracy of the integrated approach is assessed by comparisons with analytical solutions and conventional finite element thermal-structural analyses. Results show that the nodeless variable thermal element yields accuracy equivalent to a higher order element but permits a common discretization with a lower order congruent structural element. The integrated element thus provides improved accuracy and efficiency of thermal stress analysis for structures with complex temperature distributions.

Nomenclature

a	surface absorptivity
A	cross sectional area
$[B_S]$	strain-displacement interpolation matrix
$[B_T]$	temperature gradient interpolation matrix
c	specific heat
$[C]$	finite element capacitance matrix
$[D]$	elasticity matrix
E	modulus of elasticity
$\{F\}_e$	finite element nodal force vector
k	thermal conductivity
$[k]_e$	thermal conductivity matrix
$[K]_e$	finite element stiffness matrix
$[K_c]_e$	finite element conduction matrix
$[K_r]_e$	finite element radiation matrix
l	length
L	finite element length
$[N]$	finite element interpolation function matrix
$[N_S]$	finite element displacement interpolation function matrix
$[N_T]$	finite element temperature interpolation function matrix
p	perimeter
q	surface heating rate
$\{Q\}_e$	finite element heat load vector

t	time
T	temperature
T_{ref}	reference temperature for zero stresses
u,v,w	displacement components
V_e	finite element volume
x,y,z	Cartesian coordinate
$\{\alpha\}$	vector of thermal expansion coefficients
ϵ	surface emissivity or strain (eq. 12)
θ	angular position, see Fig. 5
σ	Stefan-Boltzmann constant, stress
σ_x	stress component
ρ	density

Subscripts

c	conduction heat transfer
e	finite element matrix or vector
q	specified surface heating
r	radiation heat transfer
S	structural
T	thermal
w	wall, see Fig. 2a

Superscript

T	transpose of a matrix
---	-----------------------

Introduction

The NASA Langley Research Center is conducting research programs for the development of structures for space transportation vehicles and large orbiting structures. Space transportation vehicles must be designed to withstand repeated exposure to the severe thermal environment of atmospheric reentry. Orbiting structures of unprecedented size must be designed to meet stringent dimensional stability requirements during long term exposure to the cyclical heating of earth orbit. Both designs require detailed thermal-structural analyses that present a significant challenge to existing analysis capabilities. A common feature of the thermal-stress analysis of both structures is conduction heat transfer combined with significant radiation heat transfer. Radiation heat transfer analysis of structures is difficult because the equations are inherently nonlinear and complex structural geometries strongly influence radiation heat exchanges.

Early developments in finite element methodology led to the expectation that the method would replace the finite difference-lumped parameter thermal analysis method for general structures because both thermal and structural analysis could be accomplished efficiently with the

finite element method. Another expectation was that a common model could be used for both thermal and structural analyses. These expectations have not been met because: (1) the finite element thermal analysis approach has not yet reached parity with the finite difference-lumped parameter method in capability and efficiency, and (2) intrinsic differences between heat transfer and structural problems often prohibit common models.

At the 21st and 22nd SDM Conferences, the authors presented an integrated thermal structural analysis approach^{1,2} which focused on finite element methodology for efficiently coupling steady state and transient linear thermal-structural analysis. The approach was motivated by several aerospace applications in which the structural temperature distribution required a model more complex than that required to determine the structural response. The integrated approach was developed for one dimensional, linear problems to demonstrate feasibility. Thermal elements were developed using a nodeless variable formulation to yield exact steady state nodal and element temperatures without requiring different discretization/modelling than the structural analysis. Although the exact thermal elements apply to several cases of one-dimensional conduction and convection of practical importance,³ the elements are of limited value in analysis of general aerospace structures particularly structures exposed to radiation heat transfer. The purpose of this paper is to demonstrate the feasibility of the integrated thermal-structural analysis approach to a more general class of problems which include radiation heat transfer.

The integrated approach employs new thermal finite elements which yield: (1) accurate nodal and element temperatures, (2) a common thermal-structural discretization, and (3) accurate thermal "loads" for a rigorous thermal-stress analysis. Step 3 is important because most finite element structural analysis programs have heretofore simply used nodal temperatures as input data and based thermal forces on average element temperatures. Incorporation of an accurate temperature distribution in computation of the thermal loads is an important step in obtaining improved accuracy.

Characteristics of integrated thermal-structural analysis with radiation heat transfer are first discussed. Next, a new one dimensional nodeless variable element applicable to general problems is presented. Consistent and lumped radiation conductance matrices are discussed. Finally, the accuracy and efficiency of the integrated approach is demonstrated by solving three examples using the conventional and integrated finite element approaches. In the first example, the accuracy of the finite element thermal solution is evaluated by comparison with an exact radiation heat transfer solution. In the second example, the accuracy of temperatures and stresses are evaluated for a one dimensional rod. In a final example, the approaches are compared for temperature and deformation solutions of a simplified orbiting space structure.

Integrated Thermal-Structural Analysis

Finite Element Analysis

Finite element (F.E.) formulations for nonlinear, transient thermal problems can be derived from the governing heat conduction equation with radiation boundary conditions by the method of weighted residuals.⁴ In general, element temperature $T(x,y,z,t)$ and temperature gradients are expressed in the form

$$T = [N_T] \{T(t)\}_e \quad (1a)$$

$$\begin{Bmatrix} \partial T / \partial x \\ \partial T / \partial y \\ \partial T / \partial z \end{Bmatrix} = [B_T] \{T(t)\}_e \quad (1b)$$

where $\{T(t)\}_e$ denotes a vector of element nodal temperatures as a function of time. For simplicity, conduction with only specified surface heating and radiation heat transfer will be considered. Finite element thermal analyses for other heat loads such as internal heat generation and surface convection are presented in references 1-2. For transient thermal analysis the equations for a typical element are

$$[C]_e \{\dot{T}\}_e + [K_C]_e \{T\}_e + [K_R]_e \{T\}_e = \{Q_q\}_e + \{Q_r\}_e \quad (2)$$

where the element matrices are expressed in terms of integrals over an element volume V_e and surface S_e . The element equations are

$$[C]_e = \int_{V_e} \rho c [N_T]^T [N_T] dV \quad (3a)$$

$$[K_C]_e = \int_{V_e} [B_T]^T [k] [B_T] dV \quad (3b)$$

$$[K_R]_e \{T_e\} = \int_{S_e} \sigma \epsilon T^4 [N_T]^T dS \quad (3c)$$

$$\{Q_q\}_e = \int_{S_e} q [N_T]^T dS \quad (3d)$$

$$\{Q_r\}_e = \int_{S_e} a q_r [N_T]^T dS \quad (3e)$$

All thermal parameters may be temperature dependent in general but are assumed constant herein. Radiating surfaces are assumed to be diffuse, gray and opaque. (Diffuse surfaces reflect incident radiation uniformly in all directions; gray surfaces emit energy independent of wave length. Opaque surfaces do not transmit or scatter radiation.) The incident radiation may be from several sources including: (1) distant directional sources (e.g., solar heating), (2) exchanges between surfaces with prescribed temperatures, and (3) exchanges between surfaces whose temperatures are unknown apriori. For simplicity only directional radiant fluxes are considered herein. The latter two possibilities require special consideration because radiation exchanges between surfaces must account for their geometrical relationship (i.e., viewfactors) and reflected

radiation energy. Methods for considering these additional complications appear in references 4-6.

The system matrices, after assembly from the element matrices, constitute a nonlinear set of equations because of the radiation heat transfer. The radiation conductance matrix $[K_r]_e$, implicitly defined by equation (3c), contains the effects of radiation and has a significant effect upon the thermal solution. The explicit form of $[K_r]_e$ can be derived by applying the Newton-Raphson method of solving nonlinear equations to eq. (2).⁴ The result, hereafter called the consistent radiation conductance matrix, is

$$[K_r]_e = 4 \int_{S_e} \sigma \epsilon T^3 [N_T]^T [N_T] dS \quad (4)$$

The T^3 term in the integrand of the preceding equation causes the radiation conductance matrix to be temperature dependent and hence nonlinear. The T^3 term also causes the evaluation of element integrals to be more difficult than linear capacitance or conduction matrices, eqs. (3a) and (3b), respectively. These additional complexities may be minimized through the use of a lumped formulation⁵ where the diagonal elements of $[K_r]_e$ are defined by

$$K_{r,ii} = 4T_i^3 \int_{S_e} \sigma \epsilon N_i dS \quad (5)$$

and the off-diagonal elements are zero; the subscript i denotes a typical row or column. This approximation has practical benefits and is similar to the lumped mass approximation used in structural dynamics or lumped capacitance approximation used in conduction heat transfer. However, since eq. (5) is an approximation, the accuracy of computed temperatures may be degraded.

In finite element structural analysis, element displacements $\{u\} = [u, v, w]^T$ are expressed as

$$\{u\} = [N_s] \{u(t)\}_e \quad (6)$$

where $\{u(t)\}_e$ denotes a vector of element nodal displacements as a function of time. Structural inertia effects are neglected, however, so that the structural analysis consists of a sequence of static analyses at selected time values in the transient response, i.e., a quasi-static analysis. The equations for a typical element with only thermal loads are

$$[K]_e \{u\}_e = \{F_T\}_e \quad (7)$$

where the element equations are

$$[K]_e = \int_{V_e} [B_s]^T [D] [B_s] dV \quad (8a)$$

$$\{F_T\}_e = \int_{V_e} [B_s]^T [D] \{\alpha\} (T(x, y, z, t) - T_{ref}) dV \quad (8b)$$

The temperature distribution used in evaluating the equivalent thermal load vector $\{F_T\}_e$ is defined by eq. (1a). The nodal force vector, eq. (8b), is computed for temperature distributions at selected

time values, consequently the structural analysis consists of a linear statics problem with multiple load vectors.

Integrated Analysis

To more fully develop the potential of the finite element method for thermal stress analysis the concept of integrated thermal-structural analysis was proposed in reference 1. The approach focuses on aerospace applications where normally the thermal model would have to be more detailed than the structural model. The objectives of the approach are to provide more efficient coupling of the thermal and structural analysis and improve the accuracy of the thermal-stress analysis. The approach is characterized by: (1) a common discretization for the thermal and structural analysis utilizing improved thermal elements to predict more detailed temperature variations, (2) fully compatible thermal and structural elements, and (3) equivalent thermal loads computed from eq. (8b) with temperature distributions from the improved thermal elements. The key to the approach is the development of new thermal elements which predict more detailed element temperature distributions while maintaining a common discretization with standard structural elements. In references 1 and 2, improved one-dimensional elements were based on interpolation functions from homogeneous and particular solutions to the governing differential equations. This approach, however, cannot generally be extended to more than one dimension or to nonlinear problems because closed-form solutions to the governing differential equation cannot be obtained. For these more general problems, approximate interpolation functions based on the nodeless variable concept are introduced. The thermal elements based on the nodeless variable formulation and characteristics (1)-(3) above are called integrated elements.

Integrated Elements

Conventional finite elements define unknown variables only at the nodes. The nodal unknowns used depend on continuity requirements for convergence of the finite element solution. To satisfy convergence requirements in heat conduction problems it is sufficient to use temperature as the nodal unknown; and in elasticity problems it is sufficient to use displacement components as nodal unknowns. In conventional elements the number of element nodes determines the order of the element interpolation functions. For instance, a one-dimensional element with two nodes permits a linear temperature variation, a one-dimensional element with three nodes permits a quadratic temperature variation, etc. The nodeless variable concept⁷ removes this limitation by adding extra unknowns as element variables to permit higher order interpolation functions. Several such variables may be associated with an element. Reference 7 notes that the physical interpretation of the nodeless variables may not be obvious.

Conventional and nodeless variable element families are compared for one dimensional thermal elements in Fig. 1. The conventional one-dimensional element uses two nodes which specifies a linear temperature distribution with unknown nodal temperatures. In the nodeless variable one dimensional element, an additional variable is introduced to permit the quadratic

temperature shown. For this nodeless variable element the temperature is expressed by eq. (1a) as

$$T(x,t) = N_0(x)T_0(t) + N_1(x)T_1(t) + N_2(x)T_2(t) \quad (9)$$

where $T_0(t)$ is an unknown time-dependent nodeless variable and $T_1(t)$, $T_2(t)$ are unknown time-dependent nodal unknowns. The nodeless variable $T_0(t)$ has temperature units, but does not represent the temperature at any point on the element. References 1 and 3 show for steady-state linear problems that T_0 can be determined apriori as a nodeless parameter for a given heat transfer problem by deriving the interpolation functions from solutions to the governing differential equation. This approach yields exact nodal temperatures and an exact variation of temperature within an element. Reference 2 used the interpolation functions from the exact steady-state finite elements to solve transient problems by regarding $T_0(t)$ as an unknown nodeless variable. Both approaches gave excellent results for predicted temperatures, and when these temperatures were utilized in the structural analysis, improved accuracy for displacements and stresses were achieved. Two disadvantages of exact interpolation functions are: (1) limited generality since closed-form exact solutions do not exist for either two or three dimensional linear conduction problems or nonlinear problems, and (2) heat load dependence making combined heat load cases difficult.

To overcome these disadvantages, the interpolation functions employed for the two node thermal element shown in Figure 1 are polynomials in a form suggested by the exact, linear conduction elements of Reference 1. The interpolation functions are,

$$\begin{aligned} N_0(x) &= \frac{x}{L} (1 - \frac{x}{L}) \\ N_1(x) &= 1 - \frac{x}{L} \\ N_2(x) &= \frac{x}{L} \end{aligned} \quad (10)$$

where $N_0(x)$ is one-fourth the interpolation function for the center node of a conventional quadratic element, and N_1 , N_2 are the interpolation functions of a conventional linear element. The interpolation functions, eq. (10), are capable of representing the same quadratic variation of temperature as the quadratic interpolation functions employed in a conventional element with three nodes. In fact, if $T_0 = 4T_3 - 2(T_1 + T_2)$ where T_3 is the temperature at the central node of a quadratic element, the interpolation functions are identical. The advantages of using eq. (10) rather than exact interpolation functions are: (1) the approach can be generalized to two and three dimensional or non-linear problems, and (2) the same interpolation functions can be used for all heat loads. The nodeless variable thermal element with these interpolations thus provides higher accuracy than a conventional linear element and is congruent with the standard two node structural element.

Element matrices for the nodeless variable thermal elements are derived from eqs. (3-4). Element matrices $[C]_e$, $[K_C]_e$ and $\{Q_q\}_e$ are the same for linear and nonlinear analyses:

$$[C]_e = \begin{bmatrix} C_{00} & C_{01} & C_{02} \\ C_{10} & C_{11} & C_{12} \\ C_{20} & C_{21} & C_{22} \end{bmatrix} \quad (11a)$$

$$[K_C]_e = \begin{bmatrix} K_{00} & 0 & 0 \\ 0 & K_{11} & K_{12} \\ 0 & K_{21} & K_{22} \end{bmatrix} \quad (11b)$$

$$\{Q_q\}_e = \begin{Bmatrix} Q_0 \\ Q_1 \\ Q_2 \end{Bmatrix} \quad (11c)$$

The remaining matrices $[K_r]_e$ and $\{Q_r\}_e$ exist only for nonlinear radiation heat transfer and are fully populated matrices like eq. (11a) and (11c), respectively. The nodeless variable radiation conductance matrix employed herein was derived from the consistent radiation matrix given in eq. (4). Element matrices are straightforward to evaluate except for the radiation conductance matrix. This integral was evaluated in closed-form using the symbolic manipulation language MACSYMA.

Finite element displacement interpolation functions, eq. (6), employ conventional nodal displacements as unknowns. Consequently element stiffness matrices computed from eq. (8a) are the same as used in conventional structural analysis. Element equivalent nodal forces are different, however, because the nodeless variable temperature interpolation functions, eq. (9), are used in the evaluation of the integral for nodal forces, eq. (8b). In general, element stresses can be computed from

$$\{\sigma\} = [D]\{\epsilon\} - [D]\{\alpha\}(T(x,y,z,t) - T_{ref}) \quad (12)$$

hence the improved temperature representation has a direct effect upon element stress variations. For the one dimensional rod element shown in Figure 1, the element stress is computed from,

$$\sigma_x = E(\frac{u_2 - u_1}{L}) - \alpha E (\frac{T_1 + T_2}{2} + \frac{T_0}{6} - T_{ref}) \quad (13)$$

Equation (13), which is based on the one dimensional nodeless variable temperature interpolation function, eq. (9), yields the constant stress required for rod element equilibrium. It can be derived directly from the rod differential equation and element temperature distribution.¹

For linear, transient heat conduction the nodeless variable approach has been extended to two dimensional elements.⁸ The principle difference between one and two dimensional elements is that the two dimensional elements use additional nodeless variables to insure continuity of temperature along edges of adjacent elements. The interpolation functions are similar to eq. (10).

Applications

The effectiveness of the integrated one dimensional nodeless variable element is demonstrated for three examples of conduction with

radiation heat transfer. The examples are: (1) steady-state thermal analysis of a rod with surface radiation, (2) steady-state thermal-stress analysis of a rod with surface radiation, and (3) transient thermal-stress analysis of a module of an orbiting space truss. The first example compares finite element computed temperatures with an analytical solution. All three examples demonstrate the relative accuracy of conventional elements with linear interpolation functions and integrated elements. In addition, the effect of consistent and lumped radiation conductance matrices on the conventional finite element solutions are compared in each example.

In the first two steady-state examples, the nonlinear equations are solved by Newton-Raphson iteration. In the third example, the transient nonlinear equations are solved by a Crank-Nicholson time integration scheme combined with Newton-Raphson iteration.

Infinite Rod with Surface Radiation

An infinite rod with surface radiation to space ($T_\infty = 0$) is shown in Fig. 2a. For steady-state heat transfer, the energy equation is

$$\frac{d^2 T}{dx^2} - \frac{\sigma \epsilon p}{kA} T^4 = 0 \quad (14)$$

and the boundary conditions are

$$\begin{aligned} T(0) &= T_w \\ \lim_{x \rightarrow \infty} T(x) &= 0 \end{aligned} \quad (15)$$

For these boundary conditions a closed form solution to eq. (14) exists:

$$T(x) = \frac{T_w}{\left[1 + \sqrt{\frac{9}{10} \frac{\sigma \epsilon p}{kA} T_w^3} x \right]^{2/3}} \quad (16)$$

Rod temperatures (Fig. 2b) were computed from: (1) the analytical solution, eq. (16), (2) a conventional finite element model with consistent radiation conductance matrices, (3) a conventional finite element model with lumped radiation conductance matrices, and (4) a nodeless variable finite element model. The finite element analysis used the same mesh of ten equally spaced elements for $0 < x < 1$. The input data used appears in reference 5. Hypothetical properties are used which yield a highly nonlinear temperature variation thereby providing a rigorous test for the accuracy of the finite element solutions. For the finite element solutions, the temperature computed from eq. (16) at $x = 1$ was used as a specified temperature. For all finite element models, the Newton-Raphson iteration method required seven iterations to converge for a maximum nodal temperature change to less than 0.1 percent. This convergence rate is representative of convergence for the other examples also.

Temperatures computed with conventional finite elements with either lumped or consistent radiation matrices show only fair agreement with the

analytical solution for $x < 0.5$. Temperatures computed by the nodeless variable elements show excellent agreement with the analytical solution for all nodal temperatures. Temperatures between nodes agree very well for $0.1 < x < 1$, but for $0 < x < 0.1$ the interpolated temperatures deviate from the analytical solution indicating the need for mesh refinement in the region of high temperature gradients. Although a graduated mesh would benefit all analyses, a mesh of 100 equal-length elements was used to permit comparison with results presented in reference 5. Analysis with 100 conventional elements (not shown) gave excellent agreement with the analytical solution. The largest error with lumped radiation matrices was 0.264%, and the largest error with the consistent radiation matrices was 0.137%. For the refined mesh, the temperature distribution predicted by the nodeless variable elements coincided with the analytical solution over the entire length with agreement to five significant figures. The example demonstrates, as expected, that the two-node nodeless variable element predicts temperature distributions with accuracy superior to the corresponding two-node linear element. These results should be expected since for the same mesh each nodeless variable element utilizes an additional unknown.

Fixed End Rod with Surface Radiation

A rod encased between two immovable walls is shown in Fig. 3a. The rod has specified end temperatures and is cooled by radiation to space ($T_\infty = 0$). The properties used are representative of aluminum space truss members. Rod temperatures were computed using conventional and integrated elements, and the results are compared in Figure 3b. To serve as a reference, temperatures were computed with a mesh of twenty conventional elements. Temperatures computed from a two element mesh of conventional and nodeless variable (integrated) elements are compared with this reference solution. The conventional elements with either lumped or consistent radiation matrices give only a fair approximation to rod temperatures similar to the preceding example. The nodeless variable elements predict the correct rod temperature for the node at $x/L = 0.5$ and give the correct temperature distribution along the rod. Figure 3b shows that additional conventional elements are needed to represent the rod temperature distribution accurately.

Rod displacements and stresses are compared in Table 1. The rod center displacement is overestimated by the two element conventional models, but two nodeless variable elements give excellent agreement with the reference solution. Similar trends are noted for the stresses. The two element conventional models overestimate the stress by from 12 to 23 percent, but the two nodeless variable elements predict the stress exactly. These results show the importance of using correct element temperature distributions in stress calculations. The superior accuracy of the rod displacement and stress produced by the integrated approach is due to: (1) the almost exact nodal temperature predicted by the thermal elements, and (2) incorporation of the improved temperature distribution in the calculation of the thermal stress.

Module of an Orbiting Space Truss

A three member module of an orbiting space truss (Fig. 4) is useful for evaluating conventional and integrated thermal-structural analysis in a problem of current research interest. A typical truss member receives solar, earth emitted and earth reflected heating and emits thermal energy to space. Member to member radiation exchanges are relatively small and are neglected. In a geosynchronous orbit solar heating predominates, and incident normal flux to a truss member varies significantly as a member changes orientation with respect to the solar flux vector. As the orbiting structure enters and emerges from the earth's shadow significant changes in incident heating occur. Member temperatures and structural deformations depend strongly on the time-dependent heating and member material and surface properties. To compare the thermal-structural analysis capabilities of the conventional and integrated elements, the truss module is assumed to have nominal properties of aluminum. The thermal-structural behavior of space trusses made of aluminum and advanced composite materials such as a graphite epoxy differ significantly. Aluminum truss members have a more non-uniform temperature distribution and a larger coefficient of thermal expansion. The integrated elements presented herein are effective for analysis of aluminum space trusses, but neither the integrated elements nor conventional elements are efficient for analysis of composite material space trusses. Temperature distributions along these truss members are so nearly uniform that an analysis employing isothermal elements is the most effective approach.¹⁰ Further details of thermal stress analysis of orbiting trusses with composite material members appear in references 11-12.

Temperature distributions for the three member truss module at a typical orbital position are shown in Fig. 5. To serve as a reference solution, a refined mesh of ten conventional elements per member was first used to compute member temperatures. Then member temperatures were computed with: (1) one conventional element per member with consistent radiation conductance matrices, (2) one conventional element per member with lumped radiation conductance matrices, and (3) one nodeless variable element per member.

The conventional elements did not give a good representation of interior member temperatures although the conventional elements with a lumped radiation matrix did predict nodal temperatures very well. The nodeless variable elements predicted member temperature distributions and nodal temperature very accurately with small deviations from the reference solution.

Histories of a typical member elongation, $u(L,t)$, for one orbit are compared (Fig. 6) for the various finite element models. The member elongation as computed from the one element per member conventional model temperature distributions show up to 44 percent deviation from the reference solution. These discrepancies arise because the linear temperature distributions predicted by the conventional elements (Fig. 5) give a poor representation of the average member temperature. The conventional element with lumped radiation matrix, for instance, predicts nodal temperatures quite well, but it gives poor elongation

predictions because it is based on average element temperatures. In contrast, since the nodeless variable elements represent temperature distributions very accurately, the elongation predicted from these temperatures shows excellent agreement with the reference solution with the largest discrepancy less than 1 percent.

The examples demonstrate the capability of the integrated approach for one dimensional elements. The use of the nodeless variable interpolation functions for the combination of conduction with radiation for steady state and nonlinear transient examples validate the potential of the approach. For other heat transfer cases, the temperature interpolation functions, eq. (9), and stress formula, eq. (13), yield similar results.

Concluding Remarks

An integrated approach for efficiently coupling thermal and stress analysis of structures with radiation heat transfer is presented. The paper focuses on applications where the thermal model would normally have to be more detailed than the structural model. An improved thermal element is developed employing a nodeless variable formulation. The element predicts more detailed temperature distributions than conventional elements while maintaining a common discretization with conventional structural elements. The more detailed temperature distribution is employed in the finite element structural analysis to produce more accurate displacements and stresses.

The integrated thermal-structural analysis approach is briefly described. Lumped and consistent formulations of the nonlinear radiation heat transfer matrix are presented and discussed. Nodeless variable element interpolation functions are presented for a one dimensional rod element. The role of the interpolation functions in the thermal-stress analysis is described.

Three one-dimensional examples of simple structures with radiation heat transfer are presented to illustrate the approach: (1) thermal analysis of an infinite rod with radiation, (2) thermal-stress analysis of a finite rod with surface radiation, and (3) thermal-stress analysis of a module of an orbiting space truss. The examples show: (1) the capability of the nodeless variable element to predict more detailed temperature variations than conventional elements, and (2) that more accurate displacement and stress predictions are produced when the improved temperatures are incorporated consistently in the structural model. For the one dimensional examples, the thermal element employed two nodes but allowed a quadratic variation of temperature by use of a nodeless variable. The two node thermal element thus permitted a common model with standard two node structural elements.

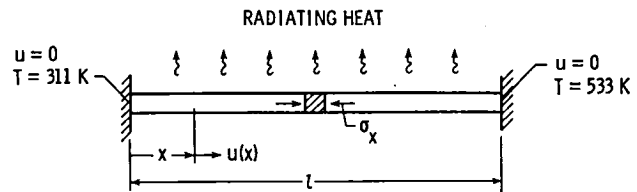
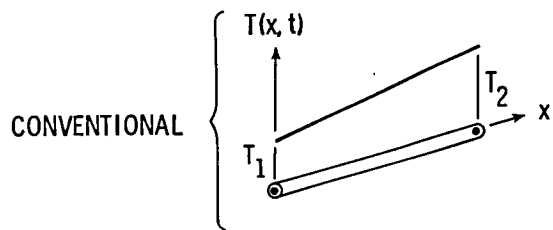
Integrated elements thus provide capability to improve accuracy and efficiency of thermal-stress analysis of structures with complex temperature distributions. The examples presented in the paper validate the approach for general one dimensional thermal stress problems but additional research is required to validate the approach for two dimensions.

References

- ¹Thornton, E. A.; Dechaumphai, P.; and Wieting, A. R.: "Integrated Thermal-Structural Finite Element Analysis." Proceedings of the AIAA/ASME/ASCE/AHS 21st Structures, Structural Dynamics and Materials Conference, Seattle, Washington, AIAA Paper No. 80-0717, May 12-14, 1980.
- ²Thornton, E. A.; Dechaumphai, P.; Wieting, A. R.; and Tamma, K. K.: "Integrated Transient Thermal-Structural Finite Element Analysis." Proceedings of the AIAA/ASME/ASCE/AHS 22nd Structures, Structural Dynamics and Materials Conference, Atlanta, Georgia, AIAA Paper No. 81-0480, April 6-8, 1981.
- ³Thornton, E. A.; Dechaumphai, P.; and Tamma, K. K.: "Exact Finite Elements for Conduction and Convection." Numerical Methods in Thermal Problems, Vol. 2 (Lewis, Morgan and Schrefler, eds.), Pineridge Press. Proceedings of the Second International Conference on Numerical Methods in Thermal Problems, Venice, Italy, July 7-10, 1981, pp. 1133-1144.
- ⁴Heubner, K.; and Thornton, E. A.: The Finite Element Method for Engineers, Second Edition, John Wiley, 1982.
- ⁵Marlowe, M. B.; Moore, R. A.; and Whetstone, W.D.: SPAR Thermal Analysis Processors Reference Manual, System Level 16. NASA CR-159162, 1979.
- ⁶Lee, H. P.; NASTRAN Thermal Analyzer, Vol. I: The NASTRAN Thermal Analyzer Manual, NASA Goddard Space Flight Center, X-322-76-16, Dec. 1975.
- ⁷Zienkiewicz, O.C.: The Finite Element Method, Third Edition, McGraw-Hill, 1977.
- ⁸Dechaumphai, P.; and Thornton, E. A.: "Nodeless Variable Finite Elements for Improved Thermal-Structural Analysis," Proceedings of the International Conference on Finite Element Methods, Shanghai, China, August 2-6, 1982.
- ⁹Siegel, R.; and Howell, J. R.: Thermal Radiation Heat Transfer, Vol. I-III, NASA SP-164, 1968.
- ¹⁰Mahaney, J.; Thornton, E. A.; and Dechaumphai, P.: "Integrated Thermal-Structural Analysis of Large Space Structures," Computational Aspects of Heat Transfer in Structures Symposium held at NASA Langley Research Center, Hampton, VA, November 3-6, 1981. NASA CP-2216, pp. 179-198.
- ¹¹Thornton, E. A.; Mahaney, J.; and Dechaumphai, P.: "Finite Element Thermal-Structural Modeling of Orbiting Truss Structures," Third Annual Technical Review Large Space Systems Technology held at NASA Langley Research Center, Hampton, VA, November 17-20, 1981. NASA CP-2215, 1982.
- ¹²Mahaney, J.; and Strode, K. B.: "Fundamental Studies of Thermal-Structural Effects on Orbiting Trusses," Student paper in proceedings of the AIAA/ASME/ASCE/AHS 23rd Structures, Structural Dynamics and Materials Conference, New Orleans, Louisiana, AIAA Paper No. 82-0605-CP, May 10-12, 1982.

Table 1 Comparative nodal displacements and thermal stress for a fixed end rod with surface radiation

Analysis Type	Disp., mm $u(x = L/2)$	Stress, kPa	Diff. in Stresses
Conventional,			
Consistent (20 F.E.)	-.35	-134.24	--
Consistent (2 F.E.)	-.40	-150.59	12.18%
Lumped (2 F.E.)	-.40	-164.77	22.74%
Nodeless Variable (2 F.E.)	-.35	-134.17	.05%



(a) ROD WITH SURFACE RADIATION

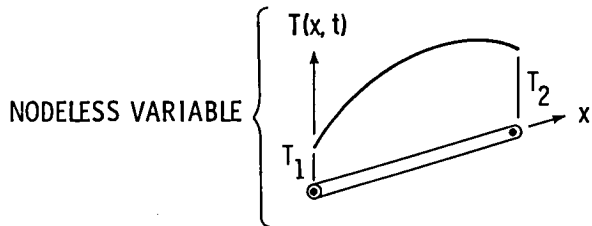
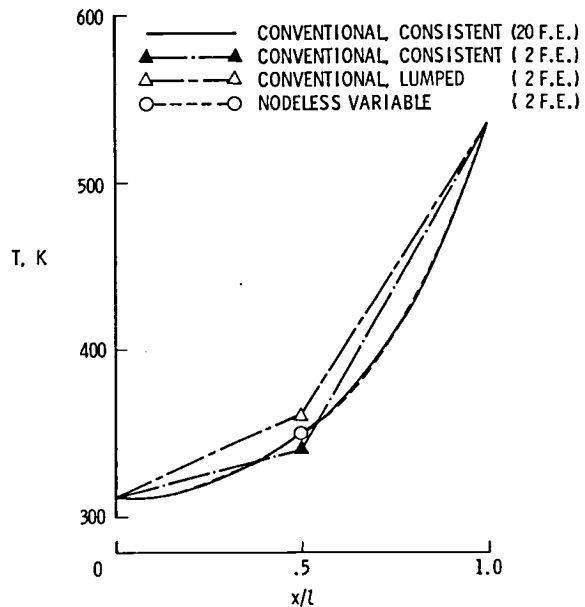
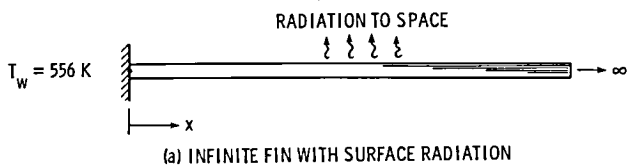


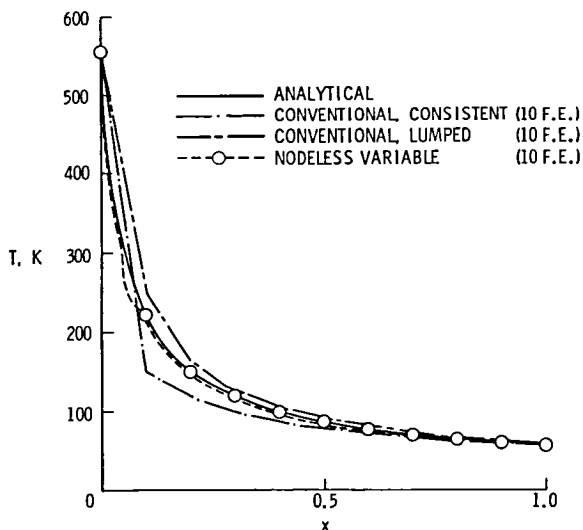
Fig. 1 Comparison of conventional and nodeless variable elements.



(b) COMPARATIVE TEMPERATURE DISTRIBUTIONS

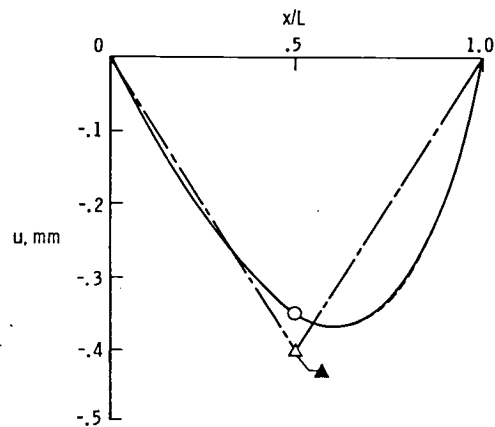


(a) INFINITE FIN WITH SURFACE RADIATION



(b) COMPARATIVE TEMPERATURE DISTRIBUTIONS

Fig. 2 Conventional and nodeless variable finite element solutions for infinite rod radiating to space.



(c) COMPARATIVE DISPLACEMENT DISTRIBUTIONS

Fig. 3 Conventional and nodeless variable finite element solutions for a fixed end rod radiating to space.

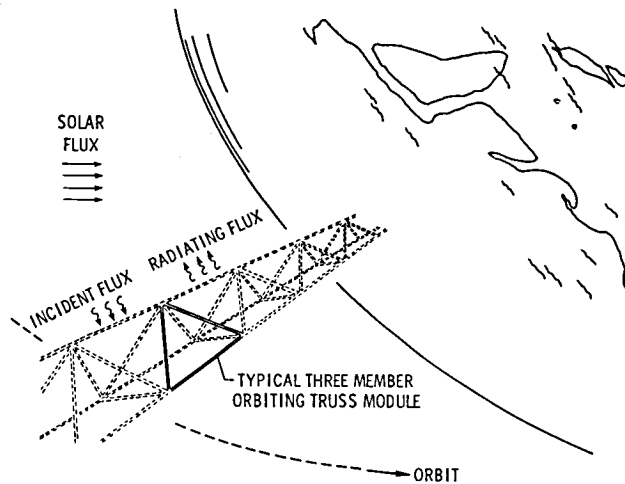


Fig. 4 Orbiting truss space structure.

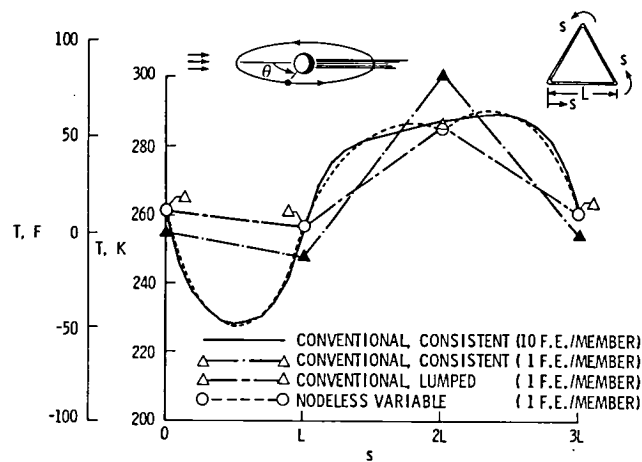


Fig. 5 Comparative temperature distribution of a three member orbiting truss at $\theta = 60$ degrees.

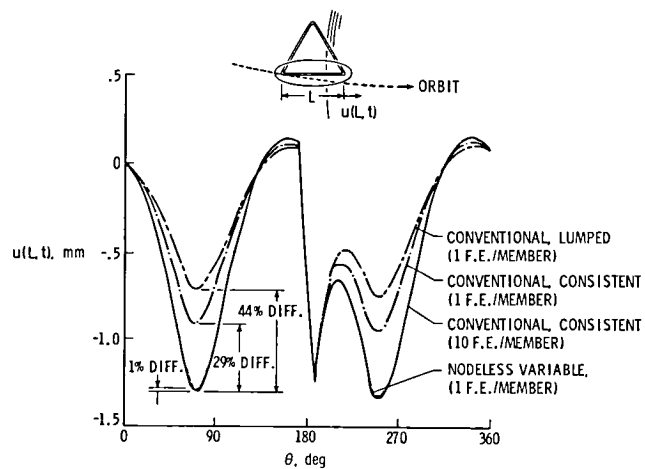


Fig. 6 Comparative displacements of a three member orbiting truss.

1. Report No. NASA TM-84469		2. Government Accession No.		3. Recipient's Catalog No.	
4. Title and Subtitle Integrated Finite Element Thermal-Structural Analysis With Radiation Heat Transfer				5. Report Date September 1982	
				6. Performing Organization Code 506-53-33-04	
7. Author(s) *Earl A. Thornton, *Pramote Dechaumphai, and Allan R. Wieting				8. Performing Organization Report No.	
9. Performing Organization Name and Address NASA Langley Research Center Hampton, VA 23665				10. Work Unit No.	
				11. Contract or Grant No.	
12. Sponsoring Agency Name and Address National Aeronautics and Space Administration Washington, DC 20546				13. Type of Report and Period Covered Technical Memorandum	
				14. Sponsoring Agency Code	
15. Supplementary Notes This paper was presented at the 23rd AIAA/ASME/ASCE/AHS Structures, Structural Dynamics and Materials Conference, May 10-12, 1982, New Orleans, Louisiana (AIAA Paper No. 82-0703) *Old Dominion University, Norfolk, Virginia					
16. Abstract An integrated approach for efficiently coupling thermal and stress analyses of structures with radiation heat transfer is presented. A new integrated one dimensional element based on a nodeless variable formulation is introduced. Lumped and consistent formulations of the nonlinear radiation heat transfer matrix are presented. The accuracy of the integrated approach is assessed by comparisons with analytical solutions and conventional finite element thermal-structural analyses. Results show that the nodeless variable thermal element yields accuracy equivalent to a higher order element but permits a common discretization with a lower order congruent structural element. The integrated element thus provides improved accuracy and efficiency of thermal stress analysis for structures with complex temperature distributions.					
17. Key Words (Suggested by Author(s)) Heat Transfer Integrated Thermal Structural Analysis Finite Element Analysis			18. Distribution Statement Unclassified - Unlimited Subject Category 34		
19. Security Classif. (of this report) Unclassified		20. Security Classif. (of this page) Unclassified		21. No. of Pages 10	
				22. Price A02	

